

Brief Reports

Brief Reports are short papers which report on completed research which, while meeting the usual Physical Review standards of scientific quality, does not warrant a regular article. (Addenda to papers previously published in the Physical Review by the same authors are included in Brief Reports.) A Brief Report may be no longer than 3½ printed pages and must be accompanied by an abstract. The same publication schedule as for regular articles is followed, and page proofs are sent to authors.

Polytope models for local icosahedral packing: An electronic structure analysis

R. B. Phillips and A. E. Carlsson

Department of Physics, Washington University, St. Louis, Missouri 63130

(Received 18 November 1987)

The electronic properties of recently developed icosahedral packing schemes using polytope $\{3,3,5\}$ (a packing of atoms on S_3 , the surface of the unit sphere in four dimensions, with perfect icosahedral symmetry) are analyzed within the framework of a d -band, tight-binding model. It is shown that there is a one-parameter family of prescriptions for defining the interatomic couplings, which preserves the icosahedral symmetry and generalizes earlier schemes. The bonding energies for several representative cases are calculated and compared to those in the fcc structure. The results are extremely sensitive to the prescription used to define the couplings.

Recent work¹⁻³ has suggested that icosahedral clusters play an important role in the structure of metallic glasses. In addition, the discovery of quasicrystals⁴ has stimulated interest in models which attach particular importance to icosahedra. Klemán and Sadoc⁵ have proposed the use of curved-space polytopes to generate locally icosahedral amorphous structures in three-dimensional Euclidean space. Polytope $\{3,3,5\}$, for example, is a generalized polyhedron constructed on S_3 , the surface of the unit sphere in four dimensions. It has 120 vertices, each with perfect icosahedral symmetry. If atoms are placed at each vertex, polytope $\{3,3,5\}$ may be taken as a model for local icosahedral packing. The curved-space polytope models are appealing because they allow one to propagate icosahedral packing without the introduction of severe packing defects, which is impossible in flat space. They also eliminate the spurious effects due to surface energies in finite-cluster calculations. Polytope $\{3,3,5\}$ has been used by Sachdev and Nelson⁶ to approximate the structure factor in glasses. The calculated structure factor exhibits the characteristic peaks observed in some metallic glasses. DiVincenzo and co-workers^{7,8} have also used polytope models to describe electronic structure in amorphous semiconductors. Widom⁹ explicitly diagonalized the s - and d -band model Hamiltonians for polytope $\{3,3,5\}$ using group-theoretic arguments, and used the electronic structure as a predictive tool in analyzing band ferromagnetism in amorphous transition metals.

In this Brief Report we generalize Widom's method by examining a range of coupling schemes which can be defined for polytope $\{3,3,5\}$ in a d -band, tight-binding

model. It is shown that this method is a special case of a one-parameter family of coupling schemes. We calculate the moments of the electronic density of states, defined by

$$\mu_n^i = \sum_{\alpha=1}^5 \langle i, \alpha | H^n | i, \alpha \rangle \quad (1)$$

where $|i, \alpha\rangle$ are atomiclike d orbitals on site i . We then use these to establish the accuracy with which the polytope can model flat-space icosahedral environments. It is found that the moments are extremely sensitive to the method for defining the couplings, and that most choices lead to moments very different from those of the flat-space icosahedron. We show that by an appropriate choice of coupling scheme, the moments up to and including the third can be made to correspond closely with those for the flat-space icosahedron. This makes it possible for the atomic environment in the first-neighbor shell to be reasonably well reproduced. Finally, we calculate the bonding energy of the polytope for three different coupling schemes. We compare these results to the bonding energy of the fcc structure to ascertain how the bonding properties differ for these various schemes.

We use a d -band, tight-binding model Hamiltonian of the form

$$H = \sum_{\substack{i,j \\ (i \neq j) \\ \alpha,\beta}} h_{\alpha\beta}^{ij} |i, \alpha\rangle \langle j, \beta|, \quad (2)$$

where i (j) are site indices, α (β) label particular atomic orbitals, and $h_{\alpha\beta}^{ij}$ is the Slater-Koster¹⁰ hopping integral. We neglect single-site terms for simplicity, since they do

not affect the results for relative structural stability. To define the couplings on the polytope, we employ the nine d -hyperspherical harmonics¹¹ which form a basis for the $n=3$ irreducible representation of $SO(4)$. These nine harmonic functions $\psi_{3LM}(\mathbf{r}_i)$ are defined at each site with respect to a local quantization axis $\hat{\mathbf{n}}_i$,¹² shown in Fig. 1.

In our Hamiltonian matrix we wish to retain only the orbitals which have d character about $\hat{\mathbf{n}}_i$. It is thus necessary to evaluate matrix elements of the form

$$\hat{\mathbf{n}}_i \langle i, L=2, M | H | j, L'=2, M' \rangle_{\hat{\mathbf{n}}_j}, \quad (3)$$

where i and j are labels describing the particular atoms being coupled, and the kets denote basis orbitals whose r dependence is not treated explicitly. Since we consider only $n=3$ we do not include a label for this quantum number in the ket. Figure 1 shows the three choices of $\hat{\mathbf{n}}_i$ and $\hat{\mathbf{n}}_j$ used in these calculations. The angle θ gives the difference in direction between the quantization axis $\hat{\mathbf{n}}_i$ ($\hat{\mathbf{n}}_j$) and the vector normal to S_3 at site i (j). We have used $\theta=0, 18^\circ$, and 36° in this work as illustrative examples, with $\theta=18^\circ$ corresponding to earlier work by Widom.⁹ The angular dependence of the couplings is contained in the difference vector $\mathbf{r}=\mathbf{r}_j-\mathbf{r}_i$, and also in the orientation of the quantization axes $\hat{\mathbf{n}}_i$ and $\hat{\mathbf{n}}_j$. $\hat{\mathbf{n}}_i$ and $\hat{\mathbf{n}}_j$ are chosen so as to have equal and opposite angles. For any given pair of nearest-neighbor atoms, the angle θ defines a one-parameter family of quantization axes which ensure that every triplet of near-neighbor atoms has the same third moment. This ensures that each site has icosahedral symmetry.

The interatomic coupling strengths were obtained in the following manner, which is similar to the conventional R^3 case.^{10,13} If the difference vector $\mathbf{r}=\mathbf{r}_j-\mathbf{r}_i$ is along the $[1,0,0,0]$ axis and the d -like orbitals are defined relative to this axis, the coupling matrix is diagonal. The couplings then have three distinct values, denoted by $\tilde{h}_{dd\sigma}$, $\tilde{h}_{dd\pi}$, and $\tilde{h}_{dd\delta}$, corresponding to different orbital character about the bond axis.

Thus, to obtain a general matrix element of the form given in Eq. (3), we use the representation matrices for $SO(4)$ to perform three distinct rotations which bring the

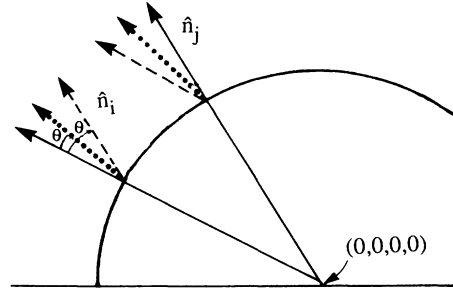


FIG. 1. Three prescriptions used to define local quantization axes for the polytope. θ is the angle between the normal at the surface and the quantization axis. Dashed line, $\theta=36^\circ$; dotted line, $\theta=18^\circ$; solid line, $\theta=0$.

difference vector and the axes defining the orbitals into coincidence with the $[1,0,0,0]$ direction. This yields a coupling which is a linear combination of the \tilde{h}_{dd} 's. First we take the hyperspherical harmonics defined with respect to the local quantization axes, and rotate them into coincidence with the fixed Cartesian R^4 axes. The rotation is carried out using the four-dimensional analog D of the 3×3 Wigner matrices. The D matrices form a representation for the rotation group $SO(4)$. We use the homomorphism¹¹ between $SU(2) \times SU(2)$ and $SO(4)$ to obtain the matrix elements of the representation. Thus

$$\begin{aligned} & |i, L=2, M \rangle_{\hat{\mathbf{n}}_i} \\ &= \sum_{L_1, M_1} D_{L_1, M_1, 2M}(A, B) |i, L_1, M_1 \rangle_{[1,0,0,0]}, \quad (4) \end{aligned}$$

where (A, B) labels the $SU(2)$ pair that effects the rotation. This is the four-dimensional analog of the transformation equation for the three-dimensional spherical harmonics under rotations. At this point we have expressed the hyperspherical harmonics at site i , defined with respect to the axis $\hat{\mathbf{n}}_i$, in terms of hyperspherical harmonics defined with respect to the $[1,0,0,0]$ axis. Thus we have

$$\begin{aligned} & \hat{\mathbf{n}}_i \langle i, L=2, M | H | j, L=2, M' \rangle_{\hat{\mathbf{n}}_j} \\ &= \sum_{L_1, M_1} \sum_{L_2, M_2} D_{L_1, M_1, 2M}^*(A_1, B_1) D_{L_2, M_2, 2M'}(A_2, B_2)_{[1,0,0,0]} \langle i, L_1, M_1 | H | j, L_2, M_2 \rangle_{[1,0,0,0]}. \quad (5) \end{aligned}$$

In order to obtain the matrix element on the right-hand side of Eq. (5) we now perform another rotation so that the difference vector is along the $[1,0,0,0]$ direction so that our coupling matrix will be diagonal. This leads to

$$\begin{aligned} \hat{\mathbf{n}}_i \langle i, L=2, M | H | j, L=2, M' \rangle_{\hat{\mathbf{n}}_j} &= \sum_{L_1, M_1} \sum_{L_2, M_2} \sum_{L_3, M_3} \sum_{L_4, M_4} D_{L_1, M_1, 2M}^*(A_1, B_1) D_{L_2, M_2, 2M'}(A_2, B_2) \\ & \quad \times D_{L_3, M_3, L_1, M_1}^*(A^{-1}, B^{-1}) D_{L_4, M_4, L_2, M_2}(A^{-1}, B^{-1}) \\ & \quad \times_{[1,0,0,0]} \langle i, L_3, M_3 | H | j, L_4, M_4 \rangle_{[1,0,0,0]} \quad (6) \end{aligned}$$

where now the difference vector in the matrix element on the right-hand side points in the direction $[1,0,0,0]$. In this

case the couplings ${}_{[1,0,0,0]} \langle i, L_3, M_3 | H | j, L_4, M_4 \rangle_{[1,0,0,0]}$ are diagonal and are given by

$${}_{[1,0,0,0]} \langle i, L_3, M_3 | H | j, L_4, M_4 \rangle_{[1,0,0,0]} = \delta_{L_3 L_4} \delta_{M_3 M_4} \tilde{h}_{dd}(L_3) \quad (7)$$

where $\tilde{h}_{dd}(0) = \tilde{h}_{dds}$, $\tilde{h}_{dd}(1) = \tilde{h}_{dd\pi}$, and $\tilde{h}_{dd}(2) = \tilde{h}_{dd\delta}$. Thus our final expression for the coupling matrix element is

$$\hat{n}_i \langle i, L=2, M | H | j, L'=2, M' \rangle_{\hat{n}_j} = \sum_{L_1 M_1} D_{L_1 M_1, 2M}^* (A^{-1} A_1, B^{-1} B_1) D_{L_1 M_1, 2M'} (A^{-1} A_2, B^{-1} B_2) \tilde{h}_{dd}(L_1), \quad (8)$$

where we have used the multiplicative properties¹¹ of the D matrices.

The $\tilde{h}_{dd\sigma}$, $\tilde{h}_{dd\pi}$, and $\tilde{h}_{dd\delta}$ were selected to reproduce eigenvalues for the flat-space dimer reasonably similar to those found in canonical band theory¹⁴ (± 1.230 , ± 0.667 , and ± 0.049 eV). For $\theta=0^\circ$, $\tilde{h}_{dd\sigma} = -1.566$ eV, $\tilde{h}_{dd\pi} = 0.729$ eV, and $\tilde{h}_{dd\delta} = -0.049$ eV; for $\theta=18^\circ$, $\tilde{h}_{dd\sigma} = -1.378$ eV, $\tilde{h}_{dd\pi} = 0.665$ eV, and $\tilde{h}_{dd\delta} = -0.049$ eV; for $\theta=36^\circ$, the parameters are the same as for $\theta=0^\circ$.

Figure 2 shows the densities of states (DOS's) for the three different choices of quantization axes, with the fcc density of states also shown for comparison. The densities of states were approximated by using six moments in the "maximum entropy" method.¹⁵⁻¹⁷ The DOS's appear very different even qualitatively. For $\theta=0^\circ$ and 18° , these DOS's bear little resemblance to those seen in typical topologically close-packed phases,^{17,18} which exhibit a single pronounced "pseudogap" rather than the two gaps seen here. As an aid in interpreting Fig. 2 we give the values of the third moment of the density of states for the flat-space icosahedron and for the three coupling schemes on the polytope: $\mu_3(\text{flat space}) = -16.91$ eV³, $\mu_3(\theta=0) = 26.25$ eV³, $\mu_3(\theta=18^\circ) = 8.17$ eV³, and $\mu_3(\theta=36^\circ) = -13.05$ eV³. The different shapes of the

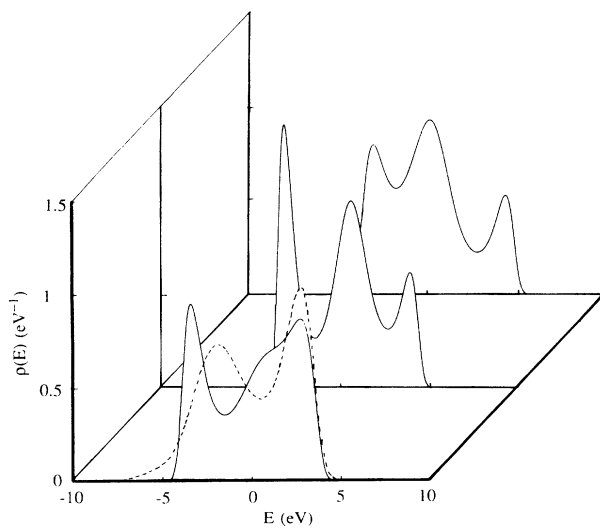


FIG. 2. DOS's per site for the three coupling schemes. Dashed line shows fcc density of states for comparison. First DOS corresponds to $\theta=36^\circ$; second DOS to $\theta=18^\circ$; third DOS to $\theta=0$.

DOS's reflect the widely different values of the moments of the DOS for them. As θ goes from 0° to 36° , we see that the DOS's change from having two dips to only one. As μ_3 becomes positive, the asymmetry of the DOS shifts from left to right. The choice of axes with $\theta=18^\circ$ (\hat{n}_i and \hat{n}_j parallel to one another, and perpendicular to the difference vector $\mathbf{r} = \mathbf{r}_j - \mathbf{r}_i$) is equivalent to earlier work by Widom,⁹ as was found by the present authors by explicitly diagonalizing the Hamiltonian using that prescription.¹⁹ It is seen that the third moment in this case is different in both sign and magnitude from that of the flat-space icosahedron. Of the three cases considered, the best value of the third moment is found for $\theta=36^\circ$ [\hat{n}_i (\hat{n}_j) given by the direction of the position vector pointing from the origin to atom j (i)].

Although the shapes of the DOS's are clearly quite sensitive to the choice of θ , one might expect that total energies, which are integrals over the DOS, would be less sensitive. To test this conjecture, we have calculated the differences in bonding energy between the polytope with the three different coupling schemes and the fcc structure. The bonding energy per atom is approximated by the one-electron sum (the factor of 2 accounts for spin degeneracy)

$$E_{\text{coh}} = 2 \int_{-\infty}^{\epsilon_f} E \rho_i(E) dE \quad (9)$$

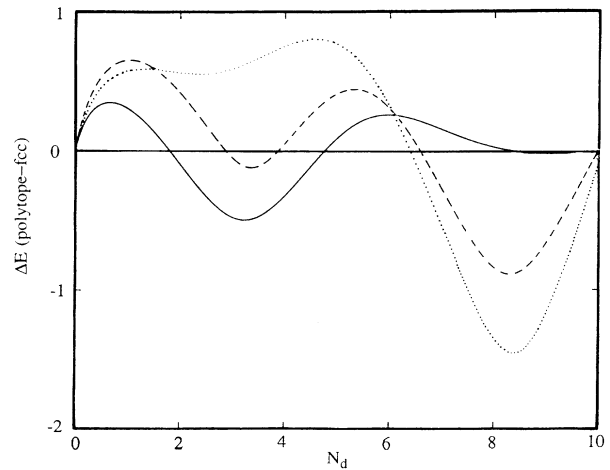


FIG. 3. Structural energy differences between polytope and the fcc structure as the number of d electrons per atom (N_d) is varied. Dotted curve, $\theta=0^\circ$; dashed curve, $\theta=18^\circ$; solid curve, $\theta=36^\circ$.

where $\rho_i(E)$ is the density of states projected on site i . In Fig. 3 we show the structural energy differences versus d -band filling to elucidate the dominant chemical trends. The structural energy differences for $\theta=0$ and $\theta=18^\circ$ exhibit an unphysically large energy scale, in comparison with typical structural energy differences, which are of order 0.5 eV.^{17,18} Furthermore, they do not display the bonding properties associated with common topologically close-packed phases like the Frank-Kasper phases,^{17,18} such as the characteristic preferability of topological close packing at about four d electrons per atom (for elemental systems).^{17,18}

In conclusion, we have seen that electronic structure calculations using polytope $\{3,3,5\}$ lead to a one-parameter family of tight-binding coupling schemes which preserve the icosahedral symmetry. If the polytope is to be used as a model for local icosahedral packing schemes in real solid environments, then special care

must be taken to choose a coupling scheme which reproduces physically reasonable values of the low-order moments. The majority of choices for these couplings lead to densities of states with little resemblance to those usually seen in topologically close-packed structures,^{17,18} such as the $A15$ structure. In this work, we have treated only the d -electron case. This case exhibits strong angular dependence of the wave functions. We might expect that properties which depend less strongly upon the angles, such as s - p electronic structure and structure factors, would be better modeled by the polytope.

The authors appreciate a helpful conversation with Michael Widom. We are grateful to Nick Papanicolaou and Lawrence Mead for the use of their maximum entropy code MAXENT. This work was supported by the Department of Energy under Grant No. DE-FG02-84ER45130.

-
- ¹J. F. Sadoc and R. Mosseri, *J. Non-Cryst. Solids* **61&62**, 487 (1984).
²D. R. Nelson, *Phys. Rev. B* **28**, 5515 (1983).
³J. P. Sethna, *Phys. Rev. B* **31**, 6278 (1985).
⁴D. Shechtman, I. Blech, D. Gratias, and J. W. Cahn, *Phys. Rev. Lett.* **53**, 1951 (1984).
⁵M. Kléman and J. F. Sadoc, *J. Phys. (Paris) Lett.* **40**, L569 (1979).
⁶S. Sachdev and D. R. Nelson, *Phys. Rev. B* **32**, 1480 (1985).
⁷D. P. DiVincenzo, R. Mosseri, M. H. Brodsky, and J. F. Sadoc, *Phys. Rev. B* **29**, 5934 (1984).
⁸M. H. Brodsky and D. P. DiVincenzo, *J. Non-Cryst. Solids* **59&60**, 101 (1983).
⁹M. Widom, *Phys. Rev. B* **31**, 6456 (1985).
¹⁰J. C. Slater and G. F. Koster, *Phys. Rev.* **94**, 1498 (1954).
¹¹J. D. Talman, *Special Functions* (Benjamin, New York, 1968).
¹²The choice of \hat{n}_i does not determine the basis functions com-

- pletely; a complete specification requires a coordinate system for each site.
¹³R. R. Sharma, *Phys. Rev. B* **19**, 2813 (1979).
¹⁴O. K. Andersen and O. Jepsen, *Phys. Rev. Lett.* **53**, 2571 (1984).
¹⁵E. T. Jaynes, in *Papers on Probability, Statistics, and Statistical Physics*, edited by R. D. Rosenkrantz (Reidel, Dordrecht, 1983).
¹⁶R. H. Brown and A. E. Carlsson, *Phys. Rev. B* **32**, 6125 (1985).
¹⁷R. B. Phillips and A. E. Carlsson (unpublished).
¹⁸P. Turchi, G. Treglia, and F. Ducastelle, *J. Phys. F* **13**, 2453 (1983).
¹⁹R. B. Phillips and A. E. Carlsson (unpublished). Using Widom's prescription for defining the couplings we explicitly diagonalized the Hamiltonian matrix rather than using the more elegant group-theoretic arguments of Widom.